



ELSEVIER

Solar Energy Materials & Solar Cells 63 (2000) 37–47

www.elsevier.com/locate/solmat

Solar Energy Materials  
& Solar Cells

# Photocurrent spectroscopy for the investigation of charge carrier generation and transport mechanisms in organic p/n-junction solar cells

Jörn Rostalski<sup>a</sup>, Dieter Meissner<sup>b,\*</sup>

<sup>a</sup>Forschungszentrum Juelich GmbH, IWV-3, D-52425 Juelich, Germany

<sup>b</sup>Nüssauer Weg 127, D-21514 Büchen, Germany

Received 7 March 1999

## Abstract

The photovoltaic behavior in a perylene/phthalocyanine hetero-p/n-junction solar cell was investigated using intensity-dependent  $I/V$ -characteristics and short circuit photocurrent spectroscopy. It is concluded that the charge carrier generation occurs only in a very thin active region at the contact. By optimizing the light trapping, a maximum solar AM 1.5 efficiency of about 2% can be obtained. A further increase requires better material properties or new cell structures. © 2000 Elsevier Science B.V. All rights reserved.

*Keywords:* Molecular organic solar cells; Photovoltaics; Organic semiconductors; Photocurrent spectroscopy; Equivalent circuit

## 1. Introduction

Organic thin films meanwhile find an increasing use in xerography [1]. Here the photoconductivity based on the concentration and mobility of majority carriers under illumination is the key process. However, when using organic materials for the production of organic solar cells [2–4] majority as well as minority carriers need to be produced and transported in the active charge generation layer. Here, the charge separation and the mobility of minority carriers will determine the width of the active

\* Corresponding author. Tel.: +49-2461-61-4053; fax: +49-2461-61-6695.

E-mail address: d.meissner@web.de (D. Meissner)

zone formed at a contact, which is producing a primary photocurrent [4,7,8]. Although the theory of electrical and optoelectrical phenomena is well understood in the case of organic crystals [5,6] there is a lack of adequate theories concerning organic thin film systems. A transfer of the theories developed for inorganic semiconductor thin films is seldom possible and useful.

In our investigations photocurrent spectroscopy has proven to be an efficient tool to determine the width of the charge generation layer formed at Schottky or p/n-type junctions. However, the understanding of the spectra obtained critically depends on the exact determination of light absorption profiles in our thin film devices that exhibit strong interference effects.

Although the width of the charge generation layer in an organic solar cell is much smaller than in an inorganic cell [7,8] high-power-conversion efficiency may be reached because of the high-absorption coefficients of the organic dyes. The sensitization solar cell that is on the verge of industrial commercialization even uses only one monolayer of an organic dye on a fractal surface to absorb the light [9].

In the following, we report on further investigations of classical Tang-type [2] organic solar cells based here on zinc phthalocyanine (ZnPc) and the methyl-substituted perylene pigment (MPP) N,N-bismethyl-perylene-3,4:9,10 tetracarboxylic acid diimide. These organic dyes have a good thermal stability, high-absorption coefficients ( $> 10^5 \text{ cm}^{-1}$ ), a sufficiently high electrical conductivity and they seem to behave like p-conducting (ZnPc) and n-conducting (MPP) materials.

## 2. Experimental

Zinc phthalocyanine (ZnPc) from Kodak and the methyl substituted perylene pigment (MPP) N,N'-dimethyl-3,4:9,10-perylene bis (carboximid) from Hoechst were purified by train sublimation. ZnPc, MPP and the contact metal were evaporated onto an ITO-coated glass substrate in a standard evaporation chamber at  $10^{-6}$  Torr. By using appropriate masks sample structures as shown in Fig. 1 were obtained.

Optical spectra of all materials as well as directly of the final cells were recorded using a Varian Cary 3 G spectrometer. The results presented in the following sections are obtained from a cell with the structure, substrate/ITO (30 nm)/MPP (20 nm)/ZnPc(220 nm)/Au (40 nm).

The short-circuit photocurrent spectra were measured using a 75 W xenon arc lamp and a monochromator. For the  $I/V$ -characteristics under illumination an AM 1.5 solar simulator (K. H. Steuernagel Lichttechnik GmbH, Mörfelden) was used. The photocurrent spectra as well as the  $I/V$ -characteristics were monitored using a Keithley SMU 236.

## 3. Experimental results

The current/voltage-characteristic of the hetero-p/n-junction solar cell under AM 1.5 illumination is shown in Fig. 2 for different light intensities. The  $I/V$ -characteristics

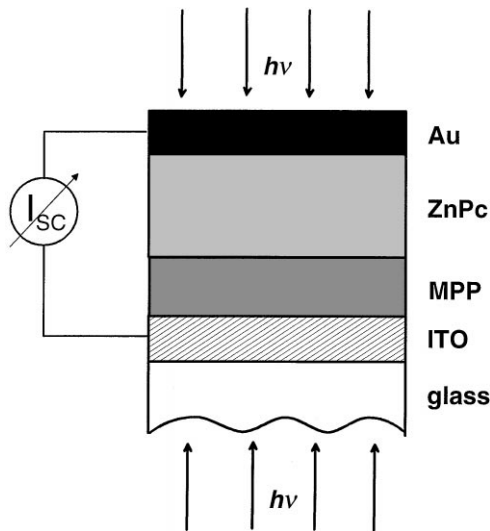


Fig. 1. Structure of a sandwich p/n-junction solar cell: substrate/ITO/MPP/ZnPc/Au.

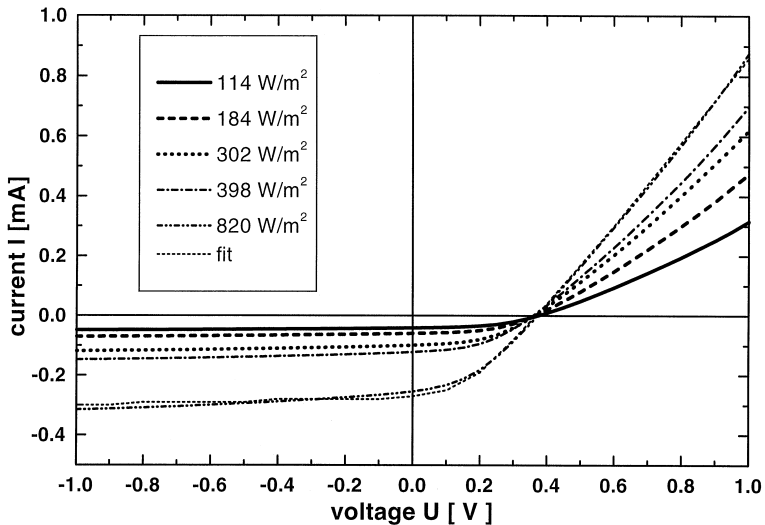


Fig. 2.  $I/V$ -characteristics of an organic solar cell under AM 1.5 illumination with different light intensities. For 820 W/m<sup>2</sup> also fitted data are plotted, see section on modeling.

of this cell show a rectifying behavior for all light intensities used. In the dark all currents are so small that they do not show up in this figure.

The characteristic quantities of the power plot, the fill factor, the short-circuit current and the power conversion efficiency have a strong dependence on the light

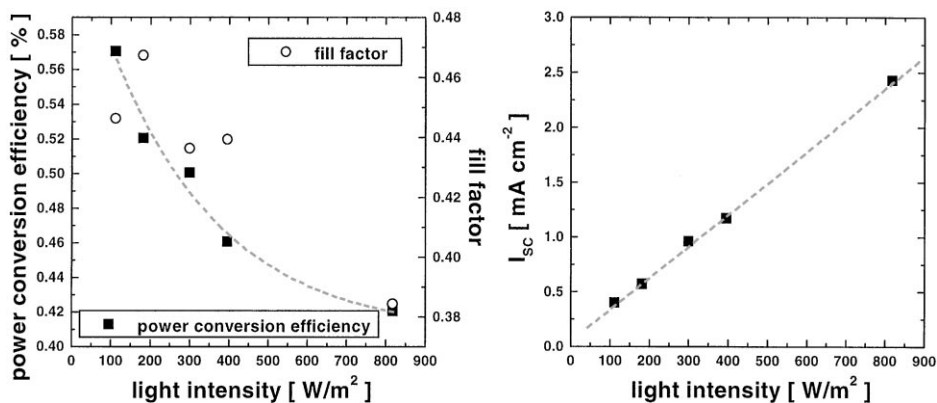


Fig. 3. Light intensity dependence of power-conversion efficiency, fill factor (left) and short-circuit photocurrent (right).

intensity (Fig. 3). The fill factor decreases with increasing light intensity. In this cell, the open-circuit voltage ( $U_{OC}$ ) did not depend on the light intensity. Therefore, also the power-conversion efficiency is decreasing with increasing light intensities.

The short-circuit current  $I_{SC}$  (Fig. 3, right) was determined to be directly proportional to the light intensity whereas the photoconductivity as measurable in strong forward polarization was found to be proportional to the square root of the light intensity for all cases investigated. This indicates that an influence of the photoconductivity on the ISC can be neglected.

The short-circuit photocurrent spectra for an illumination through the ITO as well as through the semitransparent gold back contact are shown in Fig. 4, respectively. In both cases,  $I_{SC}(\lambda)$  follows mainly the absorption coefficient of the backward, not primarily illuminated dye layer.

From this, it is obvious that the short-circuit photocurrent is generated close to the interface region of the two organic dyes (cf. Refs. [4,7,8]). If photons also absorbed far away from the interface region would contribute to the  $I_{SC}$ , we would expect a short-circuit photocurrent following the absorption spectra of both dyes. Also, in this case the shape of the  $I_{SC}$  would be identical for both directions of illumination.

## 4. Modeling

### 4.1. $I/V$ -characteristics

The  $I/V$ -characteristics (Fig. 2) can be understood on the basis of an equivalent circuit as given in Fig. 5.

The equivalent circuit consists of a series resistance  $R_S$  which is the sum of all single-layer resistances ( $R_S = R_{Au} + R_{ZnPc} + R_{MPP} + R_{ITO}$ ), a shunt resistance  $R_{SH}$ , a photogenerator  $I_{PH}$  and the diode itself. The diode behavior is described by the

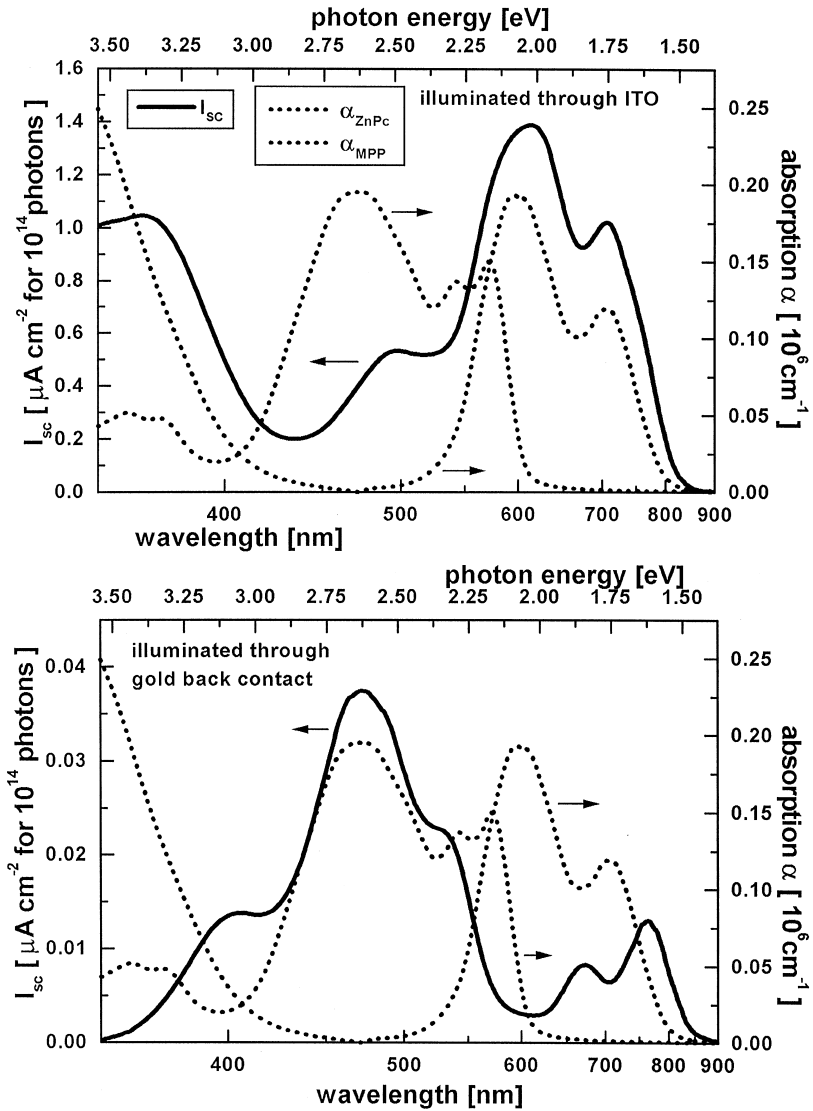


Fig. 4. Experimental short-circuit photocurrent spectra (left axis) and absorption coefficients (right axis) for frontside (top) and backside illumination (bottom) of the cell.

well-known Shockley equation. The shunt resistance accounts mainly for shorts within the p/n-junction.

Using this equivalent circuit an equation for the total current  $I$  as a function of applied voltage can easily be derived (Eq. (1)):

$$I \left( 1 + \frac{R_S}{R_{SH}} \right) - \frac{U}{R_{SH}} + I_{PH} = I_0 \left( \exp \left( \frac{e}{nkT} (U - IR_S) \right) - 1 \right), \quad (1)$$

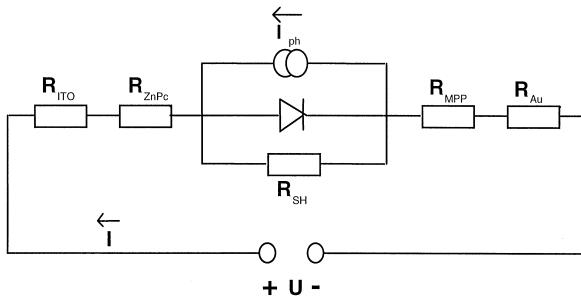


Fig. 5. Equivalent circuit of a molecular organic solar cell.

where  $I_0$  represents the saturation current density,  $n$  the ideality factor,  $k$  the Boltzmann constant and  $T$  the temperature. This transcendental equation can be solved numerically.

The  $I/V$ -characteristics under AM 1.5 illumination with a light intensity of  $820 \text{ W/m}^2$  was simulated using the described equivalent circuit and is also plotted in Fig. 2 (dotted line). The current  $I$  was calculated for a given voltage  $U$ . The parameters of the equivalent circuit were varied until the deviations between experimental and simulated data were minimized. This was the case for  $R_S = 68 \Omega$ ,  $R_{SH} = 1.5 \text{ k}\Omega$ ,  $I_0 = 50 \text{ nA}$ ,  $n = 1.4$  and  $I_{PH} = 2.4 \text{ mA}$ . The sample area was normalized to  $1 \text{ cm}^2$  for this simulation.

The open-circuit voltages of the experimental  $I/V$ -characteristics seem to be constant for the investigated light intensity regime. Therefore, it is not possible to fit the curves for the other light intensities by only changing the value of the short-circuit photocurrent in the equivalent circuit.

The equivalent circuit has to be extended in a way that it is capable to explain a constant open-circuit voltage for varying short-circuit currents. This extension is still under investigation.

#### 4.2. Short-circuit photocurrent spectra

In the experimental section we have already pointed out that a comparison of the absorption coefficients and the spectral shape of the  $I_{SC}$  has lead us to the assumption of small active regions at the organic/organic interface.

For a simulation of the short-circuit photocurrent we use a box model as illustrated in Fig. 6. This is in contrast to the generally accepted exciton diffusion model as already elaborated by Gosh and Feng [12] (cf. Ref. [4]). However, independently performed fluorescence quenching as well as electroabsorption measurements [13] support this space-charge region-based assumption.

The widths of the active regions on both sides of the contact (at  $z = 0$ ) are  $L_{MPP}$  and  $L_{ZnPc}$ , with  $d_{MPP}$  and  $d_{ZnPc}$  being the total layer thicknesses of the organic dye films. This model corresponds to a classical p/n-junction of semiconductors with a comparatively low-diffusion length, with the  $d$ 's being the thicknesses of the depletion layers.

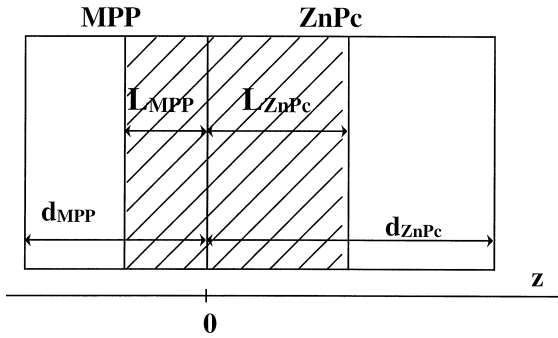


Fig. 6. Illustration of the box model, see text.

In our model [8] all photons absorbed within the active region contribute to the short-circuit photocurrent with a probability of unity. The photons absorbed in the non-active regions will not contribute to  $I_{SC}$ . As a first approximation, the effect of these absorbed photons on the photoconductivity will be neglected in the following considerations.

For a quantitative simulation of the photocurrent spectrum the total amount of photons absorbed within the active regions has to be determined for every single wavelength. The light propagation in the system substrate/ITO/MPP/ZnPc/Au is calculated using the transfer-matrix method [10] to get the complex electrical field strengths,  $E_k$  and the time averaged Poynting vector  $\langle S_k \rangle(z)$ . The negative derivative of the time-averaged Poynting vector is a measure of the absorbed light  $A(z)$ , at every position inside the dye layers (Eq. (2)).

$$\begin{aligned}
 A(z)dz &= -\frac{\partial \langle S_k \rangle(z)}{\partial z} dz \\
 &= \frac{2\pi kn}{c\mu_0 \lambda} \left[ (E'_k + E''_k) \exp\left(-\frac{4\pi k}{\lambda} z\right) + (E'_k - E''_k) \exp\left(-\frac{4\pi k}{\lambda} z\right) \right] dz \\
 &= \frac{4\pi kn}{c\mu_0 \lambda} \left[ (E'_k E''_k - E'_k E''_k) \sin\left(-\frac{4\pi n}{\lambda} z\right) + (E'_k E'_k + E''_k E''_k) \cos\left(-\frac{4\pi n}{\lambda} z\right) \right] dz.
 \end{aligned} \tag{2}$$

For an accurate calculation of Eq. (2), we have to determine the actual optical constants ( $n, k$ ) of the dyes first. The optical constants show a strong dependence on the substrate type and the growth conditions. Therefore, the optical constants and also the layer thicknesses were determined by fitting the experimentally determined optical reflectivity and transmission spectra of the whole multi-layer system. By using Eq. (2), we get the intensity and absorption profiles. In Fig. 7 these profiles are shown for four selected wavelengths for illumination from the ITO side. The profiles were also calculated for illumination through the gold back contact not shown here.

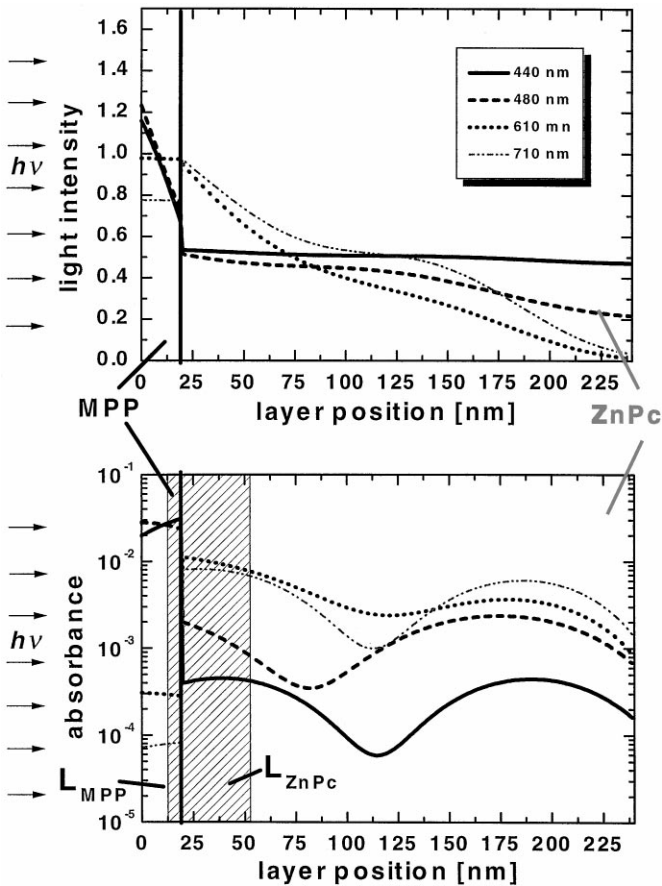


Fig. 7. Light intensity (a) and absorption profiles (b). Illumination through the ITO side.

The profiles show the described strong deviation from the Lambert-Beer-behavior (i.e. a linear decrease of the intensity on our logarithmic scale) due to strong interference effects. A summation of all photons absorbed within the striped region in Fig. 7 results in the  $I_{SC}$  for every wavelength. In our box model the widths of the active regions are the only free parameters to fit the experimentally determined absolute current values. This rather simple model is capable to explain the experimental data (Fig. 4) quantitatively.

The best correspondence between the experiment and the simulation is obtained for the case shown with  $L_{MPP} = 1$  nm and  $L_{ZnPc} = 5$  nm (Fig. 8).

The rather small width of the active region leads to a small ratio of its thickness to the total layer thickness. Therefore, a rather thick film of unused but light absorbing and low-conductive material exists and leads to unwanted efficiency losses.

In order to decrease the negative influence of the dead bulk material, we have to decrease the total layer thickness down to a value where the whole organic material is

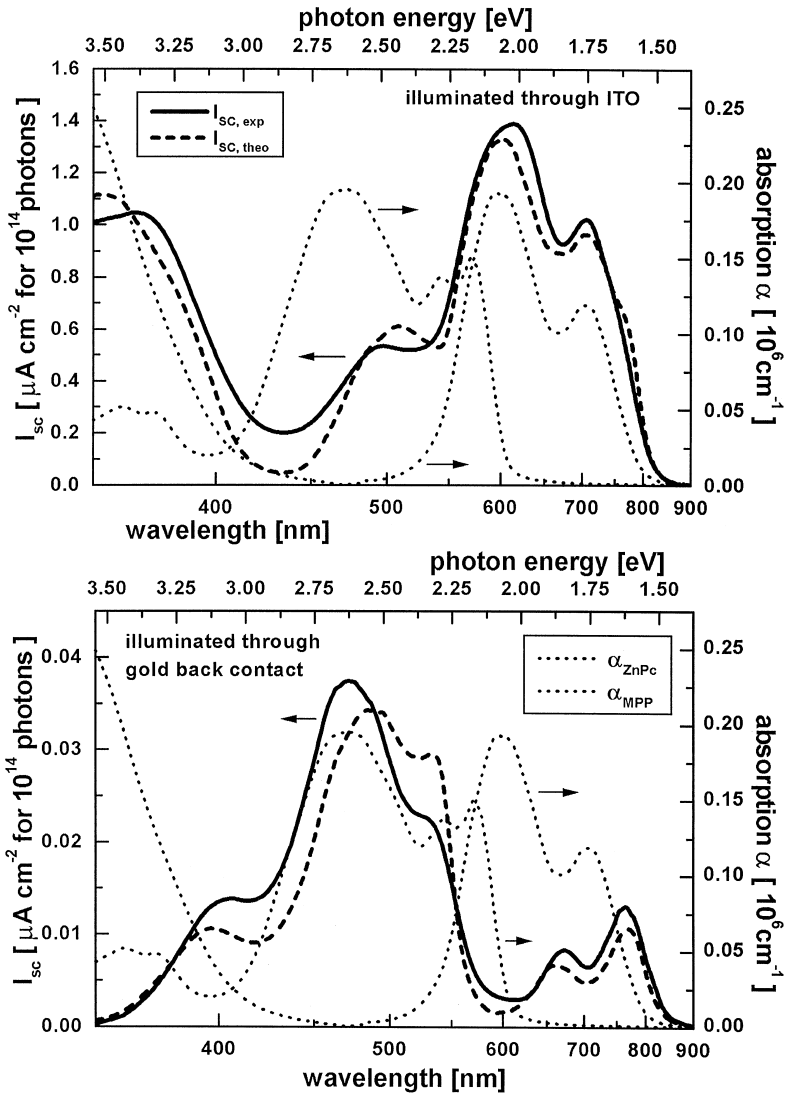


Fig. 8. Comparison of the experimental and simulated ( $L_{MPP} = 1 \text{ nm}$  and  $L_{ZnPc} = 5 \text{ nm}$ ) short-circuit photocurrent spectra (left axis) and absorption coefficients (right axis).

active. Fig. 9 shows the simulated  $I_{SC}$  upon AM 1.5 illumination for a cell system substrate/ITO (30 nm)/MPP (1 nm)/ZnPc (5 nm)/Au (40 nm).

Also shown in Fig. 9, is the case for which theoretically we introduced a dielectric, non-absorbing but well-conductive layer between the ZnPc and the gold in order to tune the coherent light superposition in the layers so that we get maximum light absorption within the dye layers. By varying its parameters we found that the

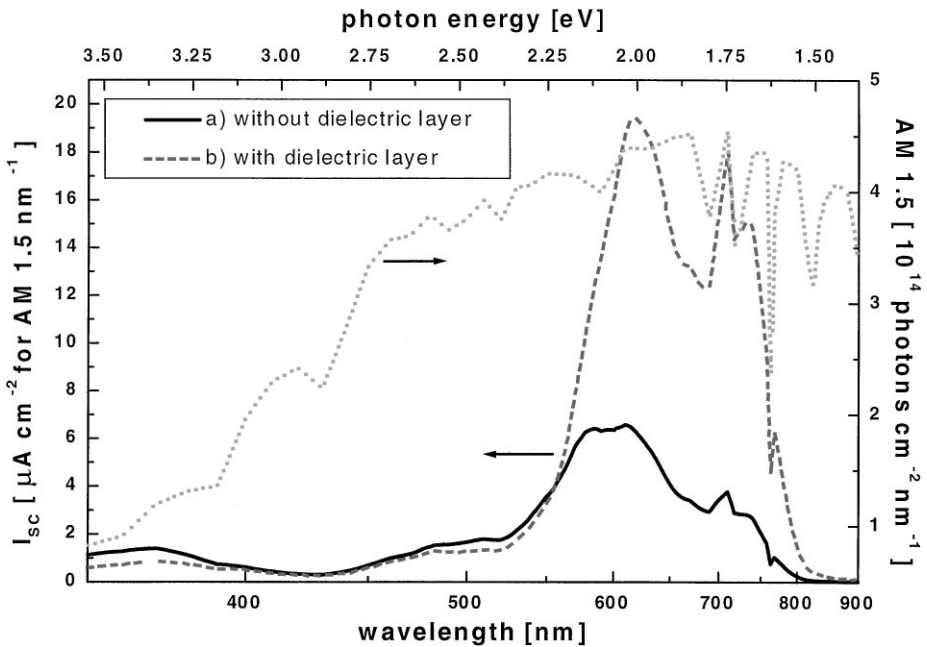


Fig. 9. Effect of an additional dielectric layer on the short circuit photocurrent  $I_{SC}$  for  $d_{MPP} = L_{MPP} = 1$  nm and  $d_{ZnPc} = L_{ZnPc} = 5$  nm.

introduction of a 60 nm thick dielectric layer with an index of refraction of 2.0 will result in an increase of the integrated  $I_{SC}$  by a factor of about 3 (Fig. 9).

If we assume an open-circuit voltage between 0.4 and 0.5 V, a fill factor of 50% and neglect all resistivity effects we would end up with a maximum power conversion efficiency of 1.9% for AM 1.5 illumination ( $820 \text{ W/m}^2$ ).

The only way to further improve the solar efficiency would be an expansion of the widths of the active regions or a new cell structure closer to that used in recent sensitization solar cells [11]. Therefore, a better control of the growth conditions and the chemical as well as the photodoping is needed.

### 5. Summary

Experimental and modeled data for an organic solar cell made from the dyes ZnPc and MPP were compared.

The  $I/V$ -characteristics shows a clearly rectifying behavior with an efficiency of about 0.5% under AM 1.5 illumination ( $820 \text{ W/m}^2$ ). The experimental short-circuit photocurrent spectrum can be simulated in terms of a p/n-junction model. The widths of the photovoltaic active regions were found to be around 1 nm in the MPP and 5 nm in the ZnPc. Therefore, only a small space-charge region at the interface of the two organic materials acts as a photocurrent generation region.

Further we estimated that an optimized light trapping by the introduction of an additional dielectric layer could result in a solar power conversion efficiency of about 1.9%.

## **Acknowledgements**

We gratefully acknowledge financial support by the European Commission under Contract no. JOR3-CT96-0106, and by the Bundesministerin für Bildung und Forschung under Contract no. 13N6906/1.

## **References**

- [1] K.-Y. Law, *Chem. Rev.* 93 (1993) 449.
- [2] C.W. Tang, *Appl. Phys. Lett.* 48 (1986) 183.
- [3] D. Wöhrle, D. Meissner, *Adv. Mat.* 3 (1991) 129.
- [4] D. Meissner, S. Siebentritt, S. Günster, Charge Carrier Generation in Organic Solar Cells, in: A. Hugot-Le Goff, C.-G. Granquist, C.M. Lampert (Eds.), *Optical Materials Technology for Energy Efficiency and Solar Energy Conversion XI: Photovoltaics, Photochemistry, and Photoelectrochemistry*, SPIE Proceedings Series Vol. 1729, Toulouse, 1992, pp. 24–35.
- [5] J. Simon, J.J. Andre, *Molecular Semiconductors*, Springer, Berlin, 1985.
- [6] M. Pope, C.E. Swenberg, *Electronic Properties of Organic Semiconductors*, Clarendon Press, Oxford, 1982.
- [7] S. Günster, S. Siebentritt, J. Elbe, L. Kreienhoop, B. Tennigkeit, D. Wöhrle, R. Memming, D. Meissner, *Mol. Cryst. Liq. Cryst.* 218 (1992) 117.
- [8] S. Günster, S. Siebentritt, D. Meissner, *Mol. Cryst. Liq. Cryst.* 229 (1993) 111.
- [9] R. Memming, *Prog. Surf. Sci.* 17 (1983) 7.
- [10] O.S. Heavens, *Optical Properties of Thin Solid Films*, Butterworths, London, 1972.
- [11] J. Desilvestro, M. Grätzel, L. Kavan, J. Moser, *J. Am. Chem. Soc.* 107 (1985) 2988.
- [12] A.K. Gosh, T. Feng, *J. Appl. Phys.* 49 (1979) 5982.
- [13] J. Rostalski, *Der Photovoltaisch aktive Bereich molekularer organischer Solarzellen*, Ph.D. Thesis, Fachbereich 1, Rheinisch Westfälisch Technische Hochschule Aachen, 1999.